ELSEVIER

Thin Solid Films 403–404 (2002) 216–222

thin solid films

www.elsevier.com/locate/tsf

Sputtered Mo/Sb_2Te_3 and Ni/Sb_2Te_3 layers as back contacts for CdTe/CdS solar cells

A.E. Abken[a,*], O.J. Bartelt[b]

[a]*Institut für Solarenergieforschung GmbH, D-30165 Hannover, Germany*
[b]*Institut für Mineralogie, Universität Hannover, D-30167 Hannover, Germany*

Abstract

A sputtered Sb–Te modification is identified as a metastable precursor phase of Sb_2Te_3. The transformation of Sb–Te into monophase Sb_2Te_3 is characterized by XRD measurements. A simple thermodynamic assessment is introduced for estimating the chemical stability of Ni/Sb_2Te_3 and Mo/Sb_2Te_3 double layers. These data and the results of kinetic test reactions for Ni/Sb–Te, Ni/Sb_2Te_3, Mo/Sb–Te and Mo/Sb_2Te_3 layers are used to provide a framework for the development of metal/telluride back contact systems for CdTe/CdS thin film solar cells with an improved long-term stability.

Keywords: Sb_2Te_3; CdTe/CdS thin film solar cells; Back contacts; Stability

1. Introduction

One key issue of manufacturing CdTe/CdS thin film solar cells is the formation of an ohmic and stable back contact. Due to the high work function of CdTe ($\Phi =$ 5.8 eV) there is no metal or alloy available to avoid the formation of a Schottky contact [1]. The best strategy to enhance ohmicity is to introduce a thin p^+-type layer between the CdTe absorber layer and the metal back contact to perform a tunnel contact [2]. Doping of CdTe is limited by the strong tendency of self-compensation [3]. Chemical etching widens grain boundaries and leaves a metastable Te-rich p^+-CdTe surface which minimizes the Schottky barrier, acts as a back surface field [4] and is necessary to form the primary contact to CdTe. The long-term stability of CdTe thin film solar cells is limited by contamination with impurities mainly originated from the back contact metal. The back contact metal diffuses easily via V_{Cd} states and along Te-rich grain boundaries through the CdTe absorber layer. A thin and dense p^+-metal telluride intermediate layer introduced as a tunnel contact acts as a diffusion barrier. It is necessary that this telluride shows a high electron affinity and creates no barrier on CdTe. Combined with Mo, low band gap p-Sb_2Te_3 satisfies these demands most and leads to an improved long-term stability of CdTe/CdS solar cells [5–9]. Sputtering as a technology for manufacturing allows the formation of stoichiometric, dense and pin-hole free Sb_2Te_3 layers.

Small stoichiometric deviations, interface states and chemical reactive transport processes, especially at the metal/telluride interface, are presumed to be responsible for contact degradation. Consuming the intermediate telluride tunnel contact layer by interdiffusion or by formation of isolated elemental and alloy precipitates embedded in the Sb_2Te_3 layer may have a significant influence on cell performance as well as chemical and electrical changes at the Sb_2Te_3/CdTe interface. Thermodynamic assessments [10–12] provide information concerning the possibility of alloy formation at the crucial metal/telluride interface. The kinetics of a presumed reaction have to be taken into account in respect of the special preparation conditions of sputtered thin films. These criteria concerning the chemical stability of metal/Sb_2Te_3 layers will provide a better understand-

* Corresponding author. Department of Physics, University of Durham, South Road, Durham DH1 3LE, UK; Tel.: +44-191-374-2395; fax: +44-191-374-7358.
E-mail address: anke.abken@debitel.net (A.E. Abken).

0040-6090/02/$ - see front matter
PII: S0040-6090(01)01527-9

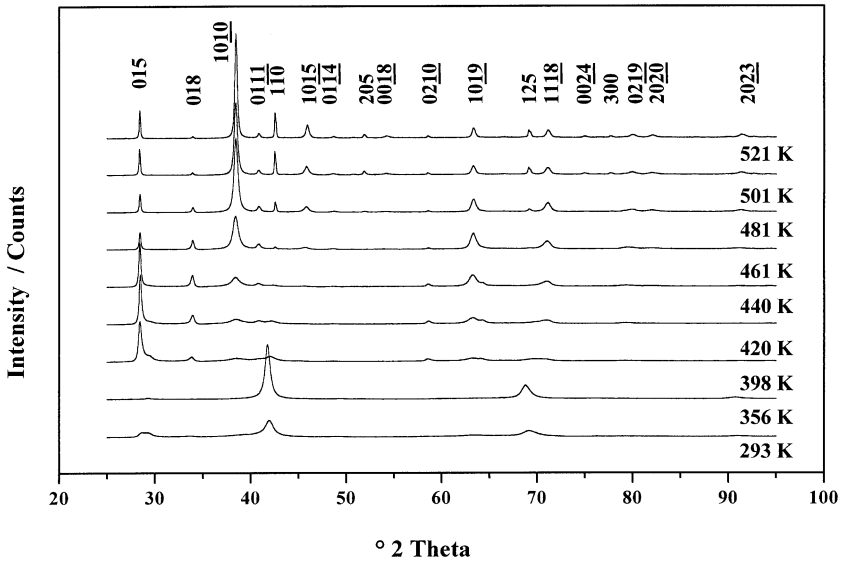

Fig. 1. XRD patterns of sputtered Sb–Te and Sb_2Te_3 layers: the substrate temperature was varied in a range of 293–521 K.

ing in view of the choice for the best suited metal for a reliable contact technology for CdTe/CdS thin film solar cells manufactured by the closed-spaced sublimation technology [13].

2. Experimental

Sb_2Te_3 and Sb–Te layers were grown on soda lime glass by DC-sputtering employing a Sb_2Te_3 target (99.99%). The substrate temperature was varied in a range of 293–521 K. For kinetic test reactions Sb–Te and Sb_2Te_3 layers deposited at 298 K and 460 K were covered with sputtered Ni (99.995%) or Mo (99.95%) layers. The kinetic test reaction samples were annealed in a nitrogen atmosphere in a temperature range of 373–573 K for 7–11 days. The samples were characterized by X-ray diffraction (XRD) measurements (Philips PW 1800) employing $CuK_{\alpha 1}$ ($\lambda = 1.54056$ Å) radiation. The XRD patterns were identified using the JCPDS data base.

3. Results and discussion

3.1. Characterization of sputtered Sb–Te and Sb_2Te_3 layers

Sputtering from a Sb_2Te_3 target at room temperature leads to a metastable Sb–Te thin film modification which is not known in Sb–Te bulk systems [12]. The structure of this Sb–Te phase is still unidentified [12] and cannot correlated with any Sb–Te compound included in the JCPDS-database. Above 398 K the Sb–Te phase transforms into monophase Sb_2Te_3 ($R\bar{3}m$) which is identified by XRD measurements (JCPDS 15-874). Raising the temperature for sputtering sharpens the peaks due to a better crystallinity of the material. The relative intensity of the 015, 018, 10$\underline{1}$0 and 110 peak changes while 10$\underline{1}$0 becomes most intense caused by the preferred orientation of Sb_2Te_3 at high substrate temperatures (Fig. 1). The lattice parameters ($a = 4.270$ Å, $c = 30.661$ Å) show slightly larger values than observed for powder samples [14].

3.2. Chemical stability of Mo/Sb_2Te_3 and Ni/Sb_2Te_3 layers

3.2.1. Thermodynamic considerations

The alloy formation at the metal/Sb_2Te_3 interface is described by simple chemical reaction equations with a defined stoichiometry. Reactions including non-stoichiometric alloys are not considered but these alloys may lead to a more favorable pathway of chemical reactions. The value of the Gibb's free energy change ΔG of a presumed chemical reaction is determined using thermodynamic data of the enthalpy changes ΔH, the entropy changes ΔS and the equilibrium constant k:

$$\Delta G = \Delta H - T\Delta S$$

$$\Delta G = -RT\ln k$$

The temperature dependence of $\Delta_T H$ and S_T is taken into account. Details of determination are described by Abken [12].

Thermodynamic data concerning the ternary systems Sb–Te–Mo and Sb–Te–Ni are summarized in Table 1. Reactions with $\Delta G > 0$ are not considered under the presumed conditions of an aged encapsulated CdTe/CdS thin film solar cell. Chemical reactions are postulated to occur spontaneously with $\Delta G < 0$ but the very special situation of a solid state reaction at interfaces of

Table 1
Thermodynamic data: Sb–Te–Ni and Sb–Te–Mo [12]

Compound/ alloy	$\Delta^\circ_f H$ (kJ mol^{-1})	S° (J K^{-1} mol^{-1})	$\Delta^\circ_f G$ (kJ mol^{-1})	C_p (J K^{-1} mol^{-1})	k_p
Sb	0	45.52	0	25.23	–/–
Te	0	49.71	0	25.70	–/–
Sb_2Te_3	−56.48	246.43	−58.35	128.72	1.7×10^{10}
Ni	0	29.87	0	26.24	–/–
NiTe	−35.65	80.12	−35.87	52.85	1.9×10^{6}
$NiTe_2$	−87.86	120.41	−85.34	76.27	8.9×10^{14}
Ni_2Te_3	−144.77	200.91	−142.58	128.10	9.5×10^{24}
NiSb	−83.68	78.24	−84.53	49.70	6.5×10^{14}
Mo	0	28.61	0	23.51	–/–
α,β-$MoTe_2$	−80.14	115.38	−76.37	76.83	2.4×10^{13}
Mo_3Te_4	−162.95	267.51	−157.84	179.54	4.6×10^{27}

sputtered polycrystalline layers has to be taken into account. However, solid state reactions may not occur for kinetic reasons even when the reaction will be possible by energetic reasons.

3.2.2. Kinetic test reactions

The value of the Gibb's free energy of the formation $\Delta^\circ_f G$ of stoichiometric Sb_2Te_3 is at standard conditions very low (−58.35 kJ mol^{-1}). For the Sb–Te phase there are no thermodynamic data available. Due to the monophase transformation into Sb_2Te_3 we have to presume that Sb–Te is less stable but we expect similar reaction products caused by chemical reactions with Mo or Ni. The morphology of the reaction zone is influenced by the nucleation rate of precipitation. Low rates will lead to a high amount of isolated phases and a dense arrangement of pores arises from the Kirkendall effect lowering the contact area of the metal/telluride interface.

3.2.3. Thermodynamic assessment and kinetic test reactions for Ni/Sb–Te and Ni/Sb_2Te_3

The main chemical reactions at Ni/Sb_2Te_3 or Ni/Sb–Te interfaces will lead to the formation of NiTe, $NiTe_2$, Ni_2Te_3 and NiSb while separating Sb or Te if we follow the formal stoichiometric equations (Fig. 2). These reactions are possible following the thermodynamic criterion of a negative value for ΔG for a spontaneous reaction and may occur while sputtering the Ni cover layer onto polycrystalline Sb_2Te_3 or Sb–Te layers. Ni will enrich the grain boundaries of Sb_2Te_3 or Sb–Te while forming these products due to its high mobility. The main reaction zone is located in the tunnel contact layer. The diffusion of Sb or Te into the Ni layer acquires a higher activation energy because Sb and Te have to be liberated from a stable lattice. Thermodynamic data concerning the most Ni-antimonides (except NiSb) are not available: these compounds are not considered in Fig. 2.

As a result of the formation of Ni-antimonides and Ni-tellurides, the liberated component will be precipitated in an elemental and reactive phase forming Ni-, Sb- and Te-alloys and solid solutions, respectively. Stoichiometric requirements cannot be satisfied exactly in a solid state system caused by different diffusion velocities of the migrating species even if these components are using the same sublattice for migration.

If we presume the temperature of an operating thin film solar cell in a range of 350–370 K, the kinetic test reaction of a double layer system annealed at 373 K is a comparable system. A Ni/Sb_2Te_3 sample annealed at 373 K for 7 days shows a XRD pattern which is identical to the pattern of an untreated sample: the XRD patterns of Ni (JCPDS 45-1027) and Sb_2Te_3 (JCPDS 15-874) are observed (Fig. 3). A significant introduction of Ni into the Sb_2Te_3 lattice has to be excluded because this will have caused a shift of the peak positions due to a lattice widening or diminishing effect. If Ni/Sb_2Te_3 double layers are annealed at 473 K the pattern of $NiTe_2$ (JCPDS 8-4) appears very clear while the 002 peak is most intense. The 10$\underline{10}$ peak is still the strongest of the Sb_2Te_3 pattern. Correlated with the reactive indiffusion of Ni into the Sb_2Te_3 layer the 015 and 018 peak decrease while broadening, but remain at the same position. These results are consistent to the thermodynamic assessment for chemical reactions between Ni and Sb_2Te_3 and demonstrate that the kinetic of the reaction favors $NiTe_2$ as a main product alloy. For samples annealed at 573 K the patterns of Ni, $NiTe_2$ and Sb_2Te_3 are observed exclusively: no other Ni-telluride or Ni-antimonide can be identified. We cannot rule out that agglomerations of Sb, Te or other alloys appear in an amorphous state embedded in the Sb_2Te_3 matrix which are undetectable by XRD measurements.

The Sb–Te phase as a metastable precursor of Sb_2Te_3 will react more easily with Ni due to the lower lattice energy: Sb and Te can be freed more easily so reactions which are less favored by energetic reasons may become more important. The kinetic test reaction of Ni/Sb–Te annealed at 373 K for 7 days show no significant changes compared to the pattern of the

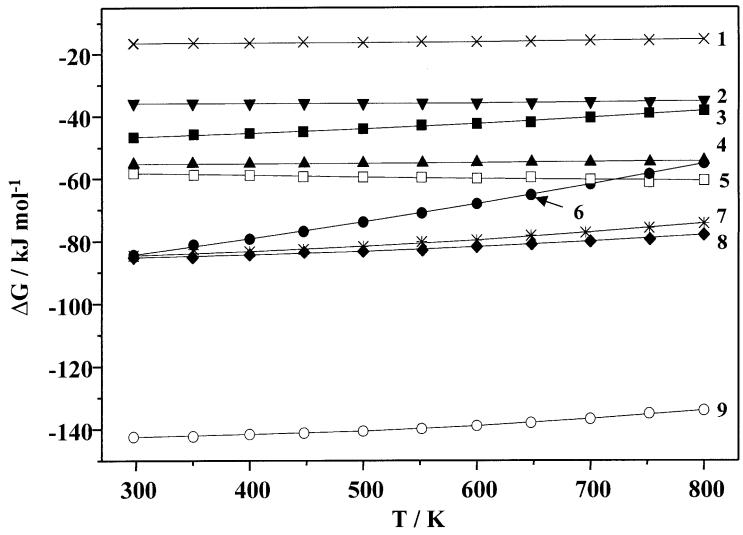

Fig. 2. Presumed reactions in the Ni/Sb_2Te_3 system: ΔG as a function of T:

1. $Ni + 1/3\ Sb_2Te_3 \rightarrow NiTe + 2/3\ Sb$
2. $Ni + Te \rightarrow NiTe$
3. $Ni + 2/3\ Sb_2Te_3 \rightarrow NiTe_2 + 4/3\ Sb$
4. $Ni + 1/2\ Sb_2Te_3 \rightarrow NiSb + 3/2\ Te$
5. $2\ Sb + 3\ Te \rightarrow Sb_2Te_3$
6. $Ni + Sb \rightarrow NiSb$
7. $2\ Ni + Sb_2Te_3 \rightarrow Ni_2Te_3 + 2\ Sb$
8. $Ni + 2\ Te \rightarrow NiTe_2$
9. $2\ Ni + 3\ Te \rightarrow Ni_2Te_3$

untreated sample: Sb–Te is still a stable modification at this temperature. The lattice parameters are not changed by the influence of Ni. The characteristic patterns of Sb_2Te_3 and $NiTe_2$ are observed if Ni/Sb–Te samples are annealed at 473 K. This leads to the conclusion that the transformation of Sb–Te into stable Sb_2Te_3 occurs without a significant incorporation of Ni in concentrations higher than a doping level in the Sb_2Te_3 bulk material. The transformation of Sb–Te into Sb_2Te_3 is finished whereas Ni is still reacting with the tunnel contact layer (Fig. 4).

3.2.4. Thermodynamic assessment and kinetic test reactions for Mo/Sb–Te and Mo/Sb_2Te_3

Thermodynamic assessments of Mo/Sb–Te and Mo/Sb_2Te_3 interface reactions lead to the conclusion that we have to expect the formation of α,β-$MoTe_2$ and Mo_3Te_4 as defined alloys (Table 1, Fig. 5) while consuming the Sb_2Te_3 spontaneously. For Mo_3Sb_7 there are no thermodynamic data available. Chemical reactions located at the interface of Mo/Sb-Te and Mo/Sb_2Te_3 double layers leading to Mo-tellurides release similar values of ΔG compared to the formation of the favored reaction products for reactions at Ni/Sb–Te and Ni/Sb_2Te_3 interfaces.

No significant changes in the XRD patterns of Mo/Sb_2Te_3 layers annealed at 373 K, 473 K and 573 K are observed: the patterns of Mo (JCPDS 4-0811) and Sb_2Te_3 (JCPDS 15-874) are identified. Due to a better crystallinity, the heat treatment sharpens the peaks of Sb_2Te_3. It is remarkable that no other compound or alloy can be identified in a crystalline state nor a lattice widening, or a diminishing effect caused by the presence of Mo is observed. If the less stable Sb–Te is used for kinetic test reactions with Mo, no XRD pattern of the presumed alloys (Fig. 5) can be found. The typical temperature-dependent transformation of the metastable Sb–Te precursor phase into Sb_2Te_3 is observed. The transformation is not influenced by the presence of Mo (Fig. 6).

These results can be explained by two reasons: (i) the diffusion velocity of Mo is not high enough to create a reaction zone which allows the formation of a detectable amount of crystalline reaction products; (ii) the presumed alloy forming reactions require high activation energies and these are not overcome by the chosen reaction conditions. As ΔG for the chemical reactions is numerically large, a small amount of these products is expected to appear in an amorphous state at Mo/Sb–Te or Mo/Sb_2Te_3 interfaces and on the surface of Sb–Te or Sb_2Te_3 grains.

3.3. Ni/Sb_2Te_3 or Mo/Sb_2Te_3 layers as back contact systems

Decreases in photovoltaic parameters of high efficiency CdTe/CdS thin film solar cells are due to shunting,

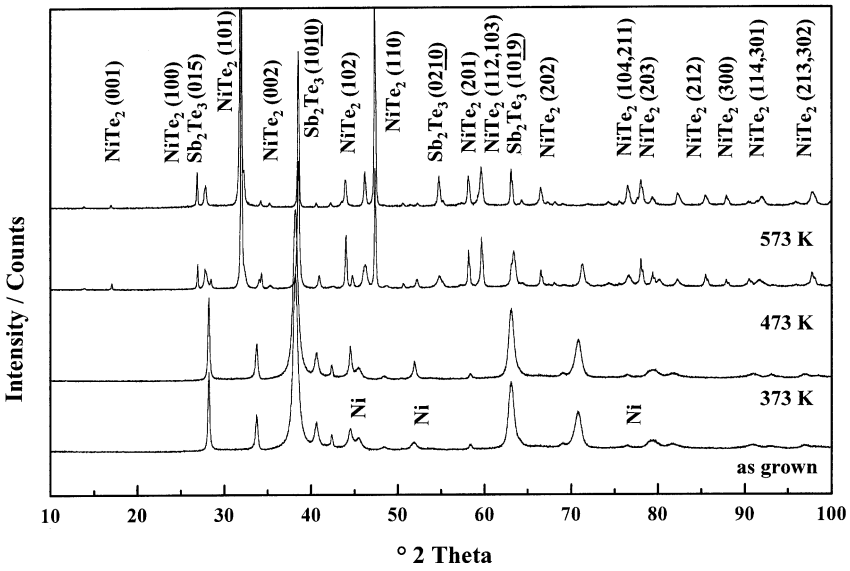

Fig. 3. Ni/Sb_2Te_3: XRD patterns of kinetic test reactions as grown and annealed in a temperature range of 373–573 K for 7 days.

junction degradation and contact degradation [15]. The degradation of the metal/tunnel contact layer system is expected to be very sensitive to small stoichiometric deviations caused by interdiffusion of the components Sb, Te, Mo and Ni, respectively. Alloy formation and changes in the doping level of the Sb_2Te_3 tunnel contact layer depend on ageing of the thin film solar cell and will change the electrical characteristics of this kind of back contact. If alloys are formed by reactive in-diffusion of the back contact metal while consuming the Sb_2Te_3, the diffusion velocity into the CdTe absorber is reduced. Liberated Sb and Te will segregate. Ni is known as a fast diffusor and due to its tendency of forming crystalline alloys while reacting with Sb–Te or Sb_2Te_3, Ni will reach the absorber layer latest when the intermediate telluride is consumed and the tunnel contact is destroyed. If Mo does not react with the tunnel contact layer, the diffusion velocity determines the appearance of the metal at the Sb_2Te_3/CdTe interface. There, Mo or Ni will meet a reactive Te-rich CdTe absorber surface: the alloy formation from the elements leading to Mo and Ni tellurides is favored by energetic reasons (Fig. 2, Fig. 5). The formation of a small amount of alloys at this primary contact interface may

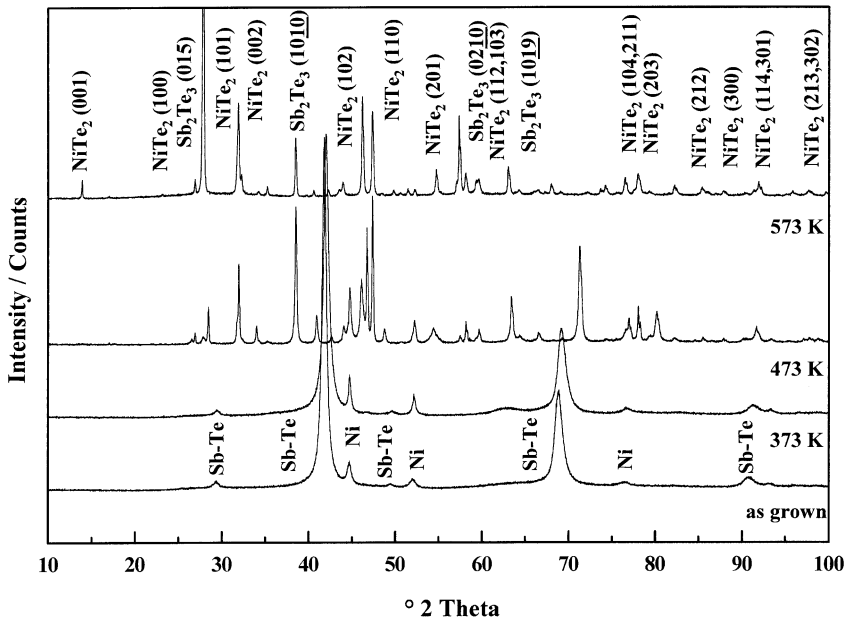

Fig. 4. Ni/Sb–Te: XRD patterns of kinetic test reactions as grown and annealed in a temperature range of 373–573 K for 7 days.

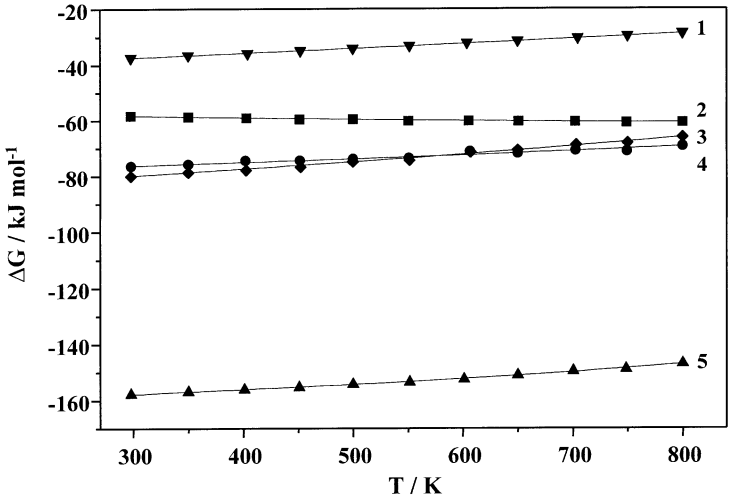

Fig. 5. Presumed reactions in the Mo/Sb_2Te_3 system: ΔG as a function of T:

1. $Mo + 2/3\ Sb_2Te_3 \rightarrow MoTe_2 + 4/3\ Sb$
2. $Sb + 3\ Te \rightarrow Sb_2Te_3$
3. $3\ Mo + 4/3\ Sb_2Te_3 \rightarrow Mo_3Te_4 + 8/3\ Sb$
4. $Mo + 2\ Te \rightarrow MoTe_2$
5. $3\ Mo + 4\ Te \rightarrow Mo_3Te_4$

be responsible for the increase in cell performance while ageing, if Mo/Sb_2Te_3 back contact systems are introduced [4,16]. If a slight amount of Mo or Ni passes the $Sb_2Te_3/CdTe$ interface, a slow cell degradation has to be expected. Deep traps, depending strongly on the chemical nature of the created defect complex, are introduced into the CdTe absorber surface and will influence the contact properties.

4. Conclusion

Sputtering at room temperature leads to a metastable Sb–Te thin film modification which is transformed into monophase Sb_2Te_3 depending on the temperature. Thermodynamic assessments of Sb–Te–Ni and Sb–Te–Mo systems lead to the conclusion that Sb_2Te_3 tunnel contacts offer no reliable chemical stability in combination

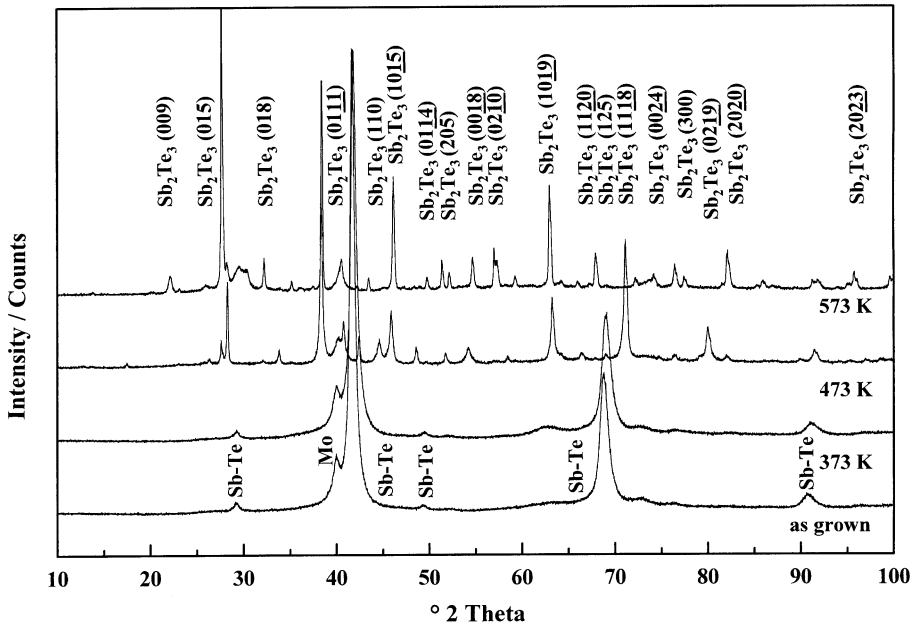

Fig. 6. Mo/Sb–Te: XRD patterns of kinetic test reactions as grown and annealed in a temperature range of 373–573 K for 7 days.

with Ni or Mo as back contact metals. Defined alloys are formed at the metal/telluride interface while consuming and destroying the Sb_2Te_3 layer. Performing kinetic test reactions, $NiTe_2$ is identified as a crystalline product by XRD measurements. The Mo/Sb_2Te_3 combination remains chemically stable while annealing due to a presumed high activation energy of the alloy formation. A slight amount of alloys in an amorphous state embedded in the Sb_2Te_3 layer and located at the Sb_2Te_3/CdTe interface will have an influence on contact stability, and therefore on cell performance. The temperature-dependent transformation of Sb–Te into Sb_2Te_3 is not influenced by Ni or Mo. Sputtered Sb_2Te_3 tunnel contacts combined with Mo will be a suitable back contact system for CdTe/CdS thin film solar cells offering an improved long-term stability.

Acknowledgements

The Bundesministerium für Bildung, Wissenschaft und Technologie BMWi (Contract No. 0329787) and the EU (Contract No. J0R39802) is acknowledged for financial support. Technical assistance was provided by Marc Köntges, ISFH, Hannover, Germany (sample preparation), and the Institute for Mineralogy, Technical University Hannover, Germany (XRD measurements). The corresponding author would like to thank Prof. Dr Nicola Romeo, Dept. of Physics, University of Parma, Italy and Dr Ken Durose, Dept. of Physics, University of Durham, UK, for stimulating discussions.

References

[1] A.L. Fahrenbruch, Sol. Cells 21 (1987) 399.
[2] B. Depuydt, M. Burgelman, M. Castelyn, A. Niemegeers, A. Verveat, Proc. 13th Eur. Conf. Photovoltaic Solar Energy Conv., Nice, 1995, p. 593.
[3] F.A. Kröger, Rev. Phys. Appl. 12 (1977) 205.
[4] D.L. Bätzner, A. Romeo, H. Zogg, R. Wendt, A.N. Tiwari, Thin Solid Films 387 (2001) 151.
[5] N. Romeo, A. Bosio, R. Tedeschi, V. Canevari, Mater. Chem. Phys. 66 (2000) 201.
[6] N. Romeo, A. Bosio, R. Tedeschi, V. Canevari, Thin Solid Films 361–362 (2000) 327.
[7] N. Romeo, A. Bosio, R. Tedeschi, A. Romeo, V. Canevari, Proc. 14th Eur. Conf. Photovoltaic Solar Energy Conv., Barcelona, 1997, p. 2351.
[8] N. Romeo, A. Bosio, R. Tedeschi, V. Canevari, Proc. 14th Eur. Conf. Photovoltaic Solar Energy Conv., Vienna, 1998, p. 446.
[9] N. Romeo, A. Bosio, R. Tedeschi, A. Romeo, V. Canevari, Sol. Energy Mater. Sol. Cells 58 (1999) 209.
[10] T. Schmidt, K. Durose, C. Rothenhäusler, M. Lerch, Thin Solid Films 361–362 (2000) 383.
[11] D.S. Boyle, K. Durose, R. Wendt, D. Bonnet, Proc. 16th Eur. Conf. Photovoltaic Solar Energy Conv., Glasgow, 2000.
[12] A.E. Abken, Sol. Energy Mater. Sol. Cells (2001) submitted for publication.
[13] A. Abken, O. Bartelt, M. Köntges, K. Oehlstrom, R. Reineke-Koch, S. Ulrich, Conf. Photovoltaic Solar Energy Conv., Glasgow, 2000.
[14] E. Dönges, Z. Anorg. Allg. Chem. 265 (1951) 51.
[15] K.D. Dobson, I. Visoly-Fischer, G. Hodes, D. Cahen, Sol. Energy Mater. Sol. Cells 62 (2000) 295.
[16] J. Beier, A.E. Abken, unpublished results.